JOURNAL OF MATERIALS SCIENCE 26 (1991) 4905–4909

Experimental study of anisothermal ageing of $(FeCoMo)_{73}$ $(SiB)_{27}$ metallic glass

A. AHAROUNE, F. A. KUHNAST, Ch. CUNAT
Laboratory of Metallurgical Thermodynamics, University of Nancy, I – U.A. CNRS 1108, B.P. 239-54506 Vandoeuvre-les-Nancy, France

Metallic glasses applied by melt spinning are always interesting alloys for their industrial applications. Among the different techniques for investigation of these glasses, we chose two complementary methods: differential scanning calorimetry and thermomechanical analysis. Correlation of the experimental results obtained with these two techniques allowed us to characterize the evolution of the $(FeCoMo)_{73}$ $(SiB)_{27}$ amorphous alloys.

1. Introduction

Metallic glasses can be obtained from liquids of appropriate concentration by quenching. If any liquid is cooled quickly enough, crystallization is prevented and the configuration of the undercooled liquid is frozen in to form a glass. Such metallic glasses possess a number of unusual properties. The metallic glass $(FeCoMo)_{73}$ $(SiB)_{27}$, supplied by Vacuumschmelze Gmbh, is used industrially for its magnetic properties [1]. As these types of non-equilibrium alloys are open to evolution, a careful study of ageing is essential to improve the industrial use of the $(FeCoMo)_{73}$ $(SiB)_{27}$ glass. It is possible to make ageing models starting from isothermal data [2–7], but this needs long experimental times. To reach the same goal, but with shorter experimental times, we attempted to obtain the same information with anisothermal measurements.

Two techniques were used: differential scanning calorimetry (DSC) and thermomechanical analysis (TMA). Our aims were the characterization of the anisothermal ageing: the determination of the crystallization apparent activation energy; and the influence of parameters such as heating rate and mechanical load.

2. Experimental procedures

2.1. Samples: elaboration and characteristics

The $(Fe\,Co\,Mo)_{73}$ $(Si\,B)_{27}$ glasses are industrial melt-spinning ribbons. With this technique ribbons of several metres (about 20 mm in width and 30 μm in thickness) can be obtained.

2.2. Apparatus

The differential fluxmetric scanning calorimeter DSC 111 Setaram works under nitrogen sweeping and is coupled to a computer, allowing both the acquisition of experimental data and their treatment. Automatic integration provided the reaction enthalpies [8]. Each experiment was conducted in two steps: firstly, heating of the amorphous substance placed in the C_1 alumina cell of the DSC (first run); and secondly, heating of the same substance formerly annealed in the C_1 cell (second run). In both cases, the C_2 reference cell was empty. By subtracting the two different thermal powers obtained during the two heatings, we deduced the thermal power linked to the evolution of the alloy.

The thermomechanical analyser TMA 40 Mettler was used. During heating, we observed the deformation of the sample under load – the system measures the length of the sample as a function of a uniaxial stress and temperature. Two types of experiments were carried out, either with a static (constant) load or with a dynamic (periodic) load. The processor gives the length expansion and the expansion coefficient. For the two types of apparatus, we used a dynamic programme of heating with a linear heating rate.

3. Results

Before any heating, the structure of the samples was examined by two methods: X ray diffusion and electron diffraction. The X ray pattern of the alloy (Fig. 1)

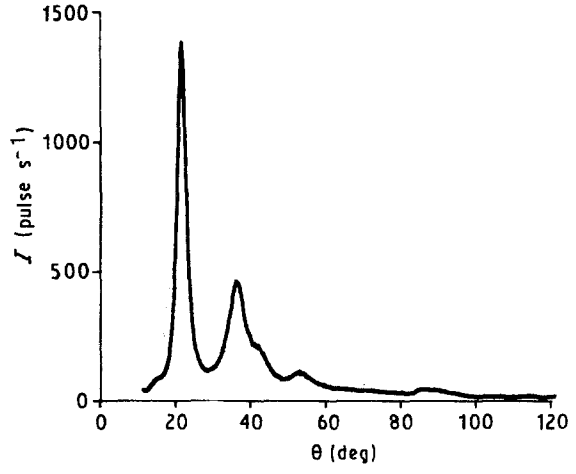

Figure 1 X-ray diffraction pattern (λMoK_α) of the as-quenched alloy.

0022–2461/91 $03.00 + .12

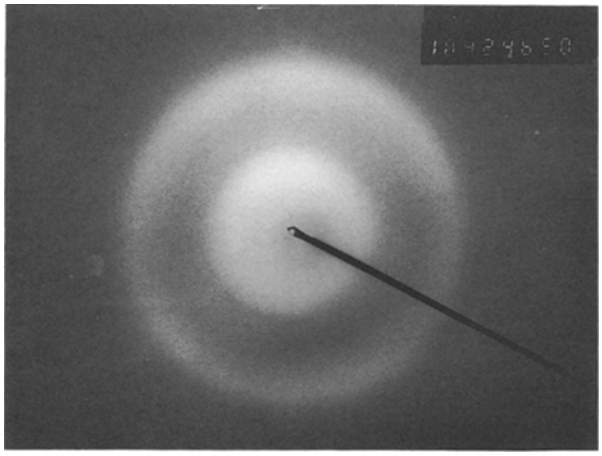

Figure 2 Electron diffraction pattern of the as-quenched alloy.

clearly shows the large rings of a typical amorphous state. It is confirmed by the electronic diffraction pattern formed of haloes (Fig. 2).

3.1. Characterization of the amorphous–crystalline transition of the alloy

To study the amorphous–crystalline transition we used the two techniques described above. For both methods the heating rate $\dot{T}$ was $10\,K\,min^{-1}$. Fig. 3 shows the apparent specific heat ΔC_p which represents the difference between the measurements of the first and the second run for annealing up to 800 °C. The thermomechanical results are presented in Fig. 4: the length expansion and the apparent expansion coefficient are plotted against temperature for the small stress $\sigma = 1.8$ MPa.

Up to the crystallization temperature T_x, samples were still amorphous, as confirmed by X ray or micrograph diffraction. This range is called the recovery or relaxation range [9]. By DSC (Fig. 3) we detected only very weak exothermic effects on the thermal power, but the corresponding enthalpy, of the order of $850\,J\,mol^{-1}$ (Table I), was not negligible. By TMA (Fig. 4) we always observed an expansion before the crystallization range. But if we compare two successive runs as for DSC, an irreversible contraction appears (about 0.022% – Table I). For a crude isotropic

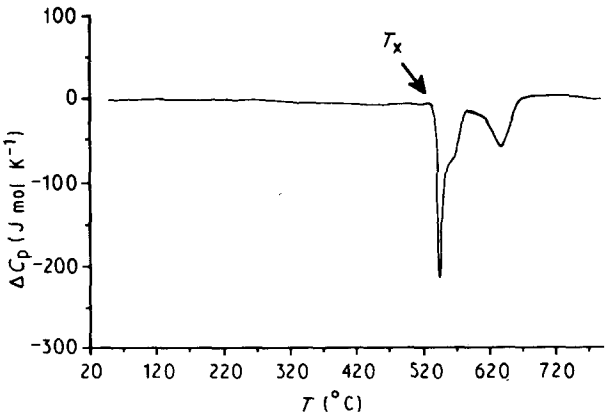

Figure 3 Apparent specific heat ΔC_p against temperature T.

TABLE I ($\dot{T} = 10\,K\,min^{-1}$)

	$\Delta L/L_0$(%)	$\Delta H(J\,mol^{-1})$
Relaxation	– 0.0219	– 850
Crystallization		
1st peak	– 0.0635	– 4300
2nd peak	– 0.1120	– 2200
Creep	40	–

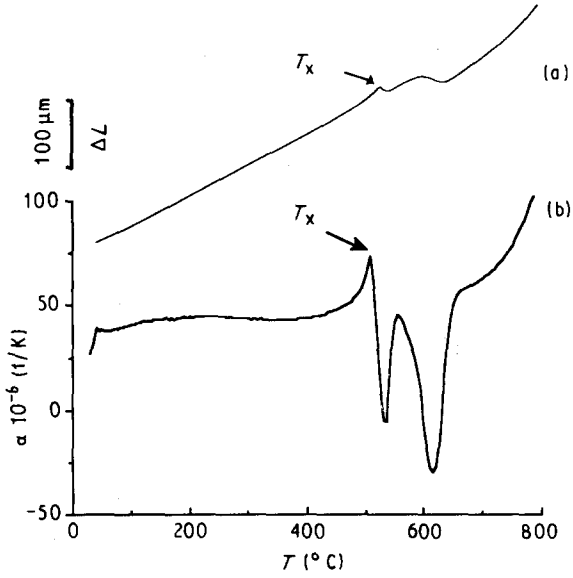

Figure 4 (a) Length expansion ΔL against temperature T; (b) apparent expansion coefficient α against temperature T.

assumption we find a decrease of the free volume of 0.066%.

After T_x, two main crystallization peaks appear in DSC experiments (Fig. 3); the corresponding enthalpy is about $-6500\,J\,mol^{-1}$ (Table I). For TMA a contraction of about – 0.17% (Table I) is observed between the onset and the end of the crystallization.

At T_A, according to Fig. 5, we observe a substantial expansion (40%, Table I). This phenomenon can be attributed to plastic creep manifestation in the crystalline state, as shown in Fig. 5.

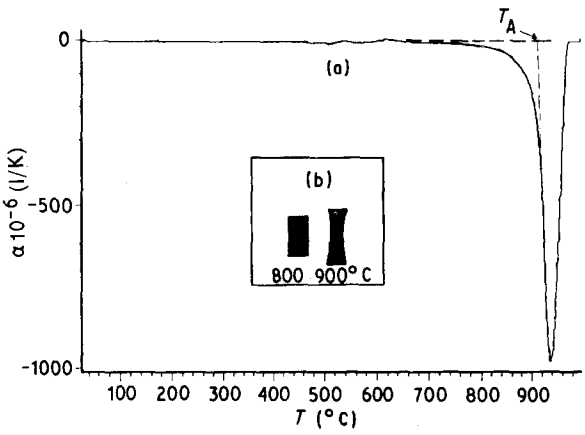

Figure 5 (a) Apparent expansion coefficient α against temperature T. T_A beginning of creep manifestation. (b) Evolution of shape of the sample against temperature T.

3.2. Determination of the apparent activation energy from DSC measurements

DSC experiments carried out at different rates, $\dot{T}$, show a shift of the peak maxima T_m (Fig. 6). T_m is an important parameter, its variation allowing the determination of the apparent activation energy of each peak. Kissinger's method [10], giving the apparent activation energy E_a can be employed to determine the real activation energy only if the considered peak is produced by a single process. Following this approach we can write

$$\frac{E_a}{R} = d\left[\ln \frac{\dot{T}}{T_m^2}\right] \Big/ d\left[\frac{1}{T_m}\right] \quad (1)$$

where E_a = activation energy; $\dot{T}$ = heating rate; and T_m = temperature of the maximum of the peak. In Fig. 7, $\ln \dot{T}/T_m^2$ against $1/T_m$ is plotted for the two peaks.

In Table II, the different apparent activation energies are reported. The activation energy is of the same order of magnitude for the two steps of crystallization.

3.3. Analysis of the DSC results for different heating rates

The relaxation enthalpies are presented in Table III. At a low heating rate, small exothermic effect appears between the two main peaks (Fig. 6), but at 10 K min^{-1}, the shoulder, present on the first peak, separates to give an independent peak (Fig. 6). These events show the complexity of the crystallization process [11, 12]. In Fig. 8, T_{m_1} and T_{m_2}, the maxima of the crystallization peak, are plotted against rate $\dot{T}$. Note the deceleration in the shift of T_{m_1} and T_{m_2} against the heating rate for $\dot{T} > 4$ K min^{-1}.

3.4. Static effect on the TMA results

Study of the length expansion Δl against the applied load, allows us to note that the position of the onset T_x and the end T_e of crystallization is not influenced by the variation of the stress in the studied stress range (Fig. 9); the creep is more important for the highest

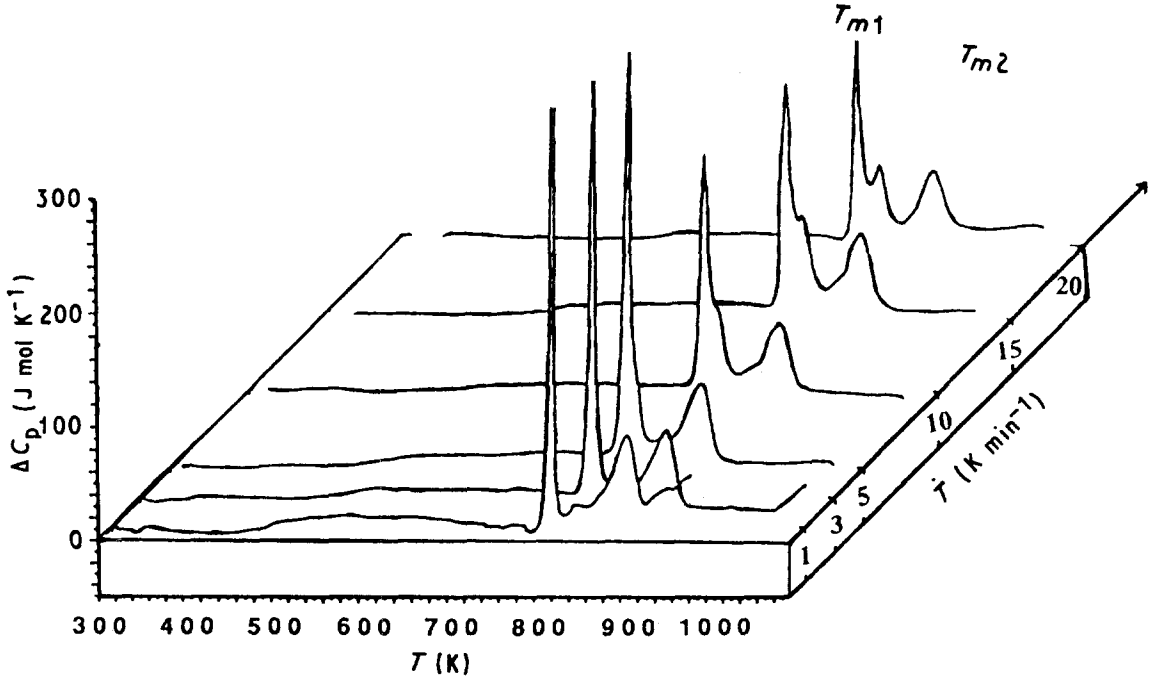

Figure 6 Apparent specific heat ΔC_p against temperature at different rates $\dot{T}$.

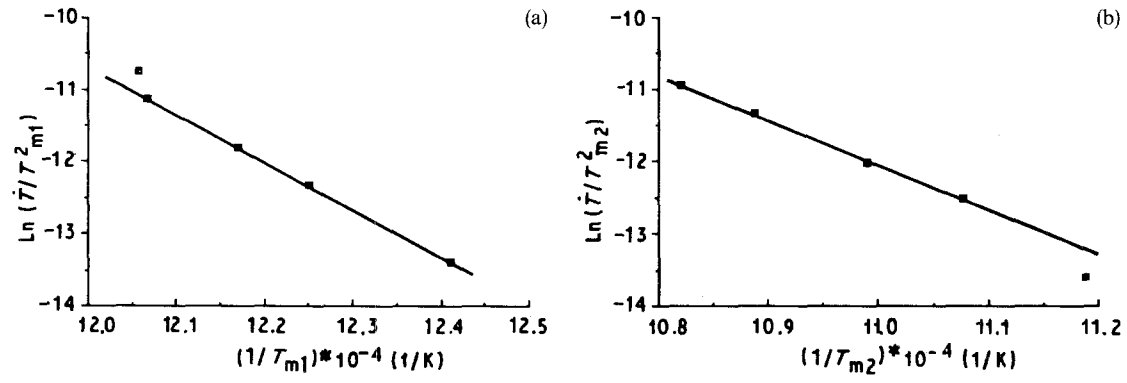

Figure 7 Apparent activation energy E_a for each crystallization peak: (a) 540, (b) 508 kJ.

TABLE II Apparent activation energies

Crystallization	E_a(kJ mol^{-1})
1st peak	540
2nd peak	508

TABLE III Relaxation enthalpies

Rate, $\dot{T}$(K min^{-1})	ΔH(J mol^{-1} K^{-1})
5	− 850
10	− 1000
15	− 1170
20	− 960

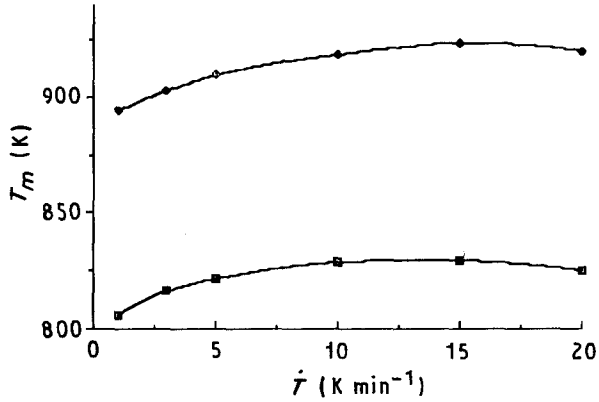

Figure 8 Temperature of the maximum of the two crystallization peaks T_m against rate $\dot{T}$. ■, T_{M_1}; ◆, T_{M_2}.

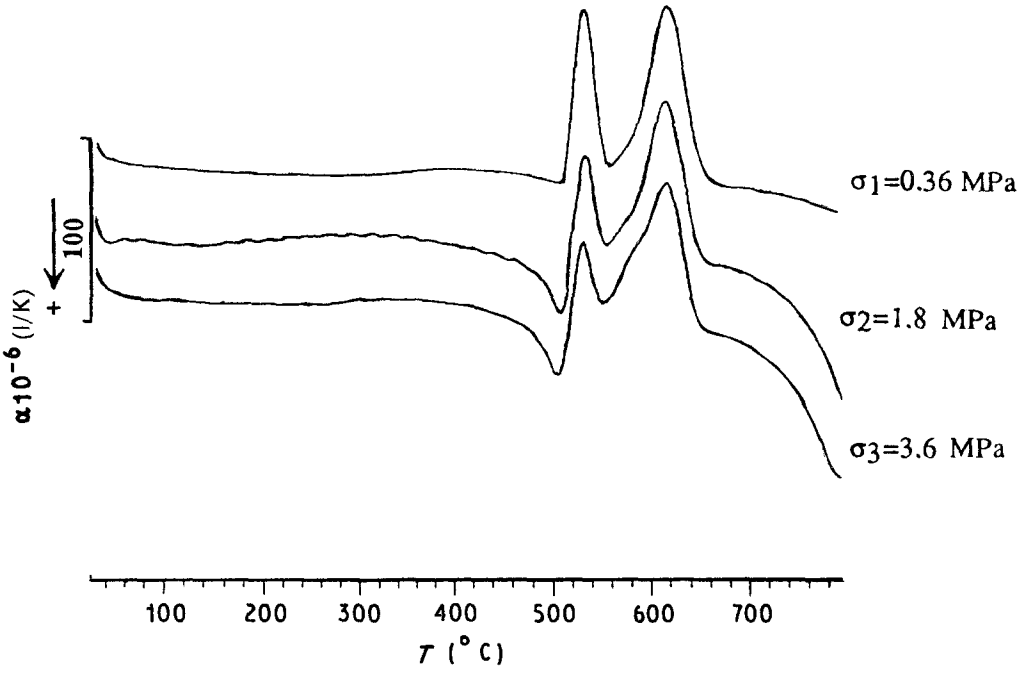

Figure 9 Apparent expansion coefficient α against temperature T for different stress σ_i.

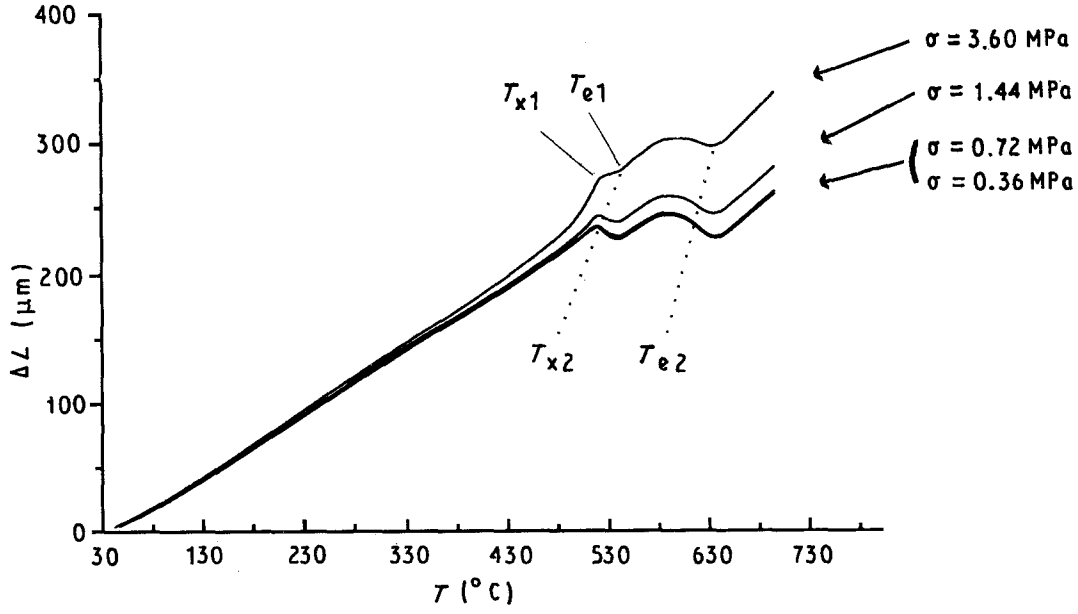

Figure 10 Length expansion Δl for the two steps of crystallization for different stress σ_i.

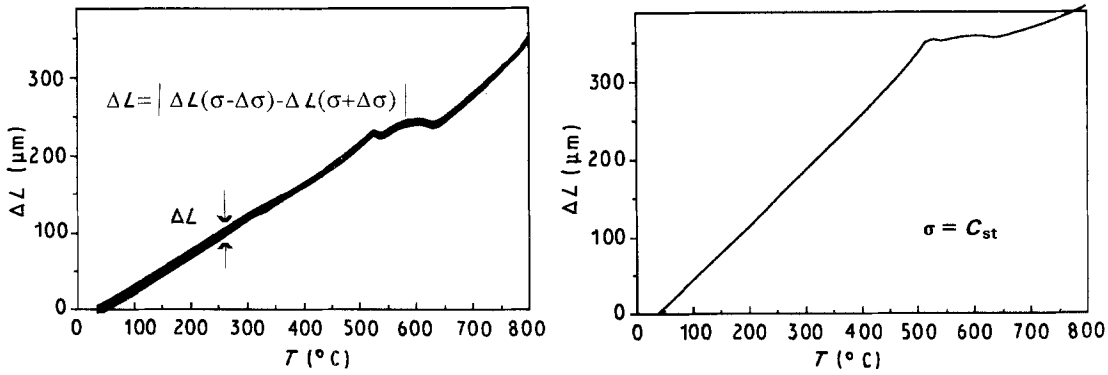

Figure 11 Length expansion Δl for cyclic and static loads against temperature T.

TABLE IV Stress effect on length expansion

F(N)	ΔL_1(μm)	ΔL_2(μm)	σ(MPa)
0.5	+ 9.26	− 6.376	3.6
0.2	− 4.87	− 14.00	1.44
0.1	− 7.74	− 18.17	0.72
0.05	− 9.04	− 18.17	0.36

loads (Fig. 9); and the sign of $\Delta l = L(T_e) - L(T_x)$ induced by each stage of crystallization increase when the load decreases (Fig. 10, Table IV).

3.5. Analysis of the TMA experiments with dynamic loads

The effects of a cyclic stress have been measured on the evolution of the sample by applying an oscillating periodic load ($F = 0.25 \pm 0.1$ N, $t = 12$ s) (Fig. 11). We observe the same effects on the length expansion ΔL as for analysis with a static load. From such experiments we calculate the ratio $\Delta l(6\,6\,0)/\Delta l(T) = E(T)/E(6\,6\,0)$ [13], where $E(T)$ is the apparent Young's modulus at T, and $E(6\,6\,0)$ is the apparent Young's modulus of the crystallized alloy at 660 °C. Fig. 12 shows an increase of the apparent Young's modulus during the relaxation.

4. Conclusions

In this paper we have characterized the anisothermal evolutions of the amorphous $(FeCoMo)_{73}$ $(SiB)_{27}$ alloy by a correlated study based on two experimental techniques, DSC and TMA. The evolution of the thermal properties shows the two classical ranges of transformations: relaxation or recovery, and crystallization [9]. By studying the rate influence we have carried out a crude kinetic analysis of the crystallization. The existence of two main peaks indicates different stages of crystallization and several processes.

The observed length contraction reveals the decrease of the free volume which is a characteristic property of the metallic glasses. We must, however, emphasize a difficulty in thermochemical analysis – the length contraction is the result of two effects, the evolution of the alloy under the effect of the temperature, and its evolution with the tensile load which induces some creep effects. Such theoretical analysis can be managed using Cunat's DNLR model [2, 13]. We are working on deducing the parameters of the DNLR model from the anisothermal data, with the aim of simulating the ageing of this alloy under complex experimental conditions.

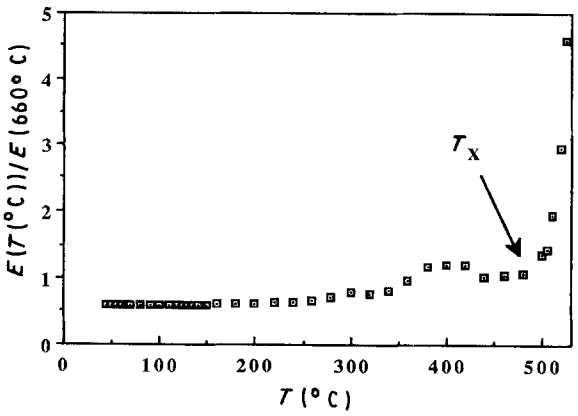

Figure 12 Evolution of the ratio of the apparent Young's modulus E at T and at 660 °C against temperature T.

Acknowledgements

We would like to thank Drs Warlimont, Hilzinger and Herzer of Vacuumschmelze Gmbh (Hanau, FRG) who gave us the samples.

References

1. G. HERZER and H. R. HILZINGER, in "Magnetic Properties of Amorphous Metals" (Elsevier, 1987) p. 354.
2. A. J. KOVACS, J. M. HUTCHINSON and J. J. AKLONIS, in "The Structure of Non-Crystalline Materials" (Taylor & Francis, London, 1977) p. 153.
3. Ch. CUNAT, *Z. Phys. Chem.* **157** (1987) 419 and 425.
4. M. A. DEBOLT, A. J. EASTEAL, P. B. MACEDO and C. T. MOYNIHAN, *J. Amer. Ceram. Soc.* **59** (1976) 16.
5. O. S. NARAYANASWAMY, *ibid.* **54** (1971) 491.
6. W. PRIMAK, *Phys. Rev.* **100** (1955) 1677.
7. M. R. J. GIBBS, J. E. EVETTS and J. A. LEAKE, *J. Mater. Sci.* **18** (1983) 278.
8. Ch. CUNAT and J. CHARLES, *Mém. Et. Sc. Rev. Mét.* **4** (1982) 177.
9. H. S. CHEN, *J. Non-Crystalline Solids* **46** (1981) 289.
10. HOMER E. KISSINGER, *Anal. Chem.* **29** (1957) 1703.
11. U. KOSTER and U. HEROLD, *Scripta Met.* **12** (1978) 75.
12. P. G. BOSWELL, *J. Mater. Sci.* **15** (1980) 1926 and 1939.
13. Ch. CUNAT, Thèse d'Etat, Nancy, France (1989).
14. M. BOUROUKBA, Thèse de l'Université de Nancy, Nancy, France (1989).

Received 19 April 1990
and accepted 15 January 1991